Investigations on Film Bulk Acoustic Wave Resonator based on Aluminum Nitride

Anubhav Jindal

A dissertation submitted for the partial fulfilment
of BS-MS dual degree in Science

Indian Institute of Science Education and Research Mohali

April 2020

Certificate of Examination

This is to certify that the dissertation titled **Investigations on Film Bulk Acoustic Wave Resonator based on Aluminum Nitride** submitted by **Anubhav Jindal** (Reg. No. MS15200) for the partial fulfillment of BS-MS dual degree programme of the Institute, has been examined by the thesis committee duly appointed by the Institute. The committee finds the work done by the candidate satisfactory and recommends that the report be accepted.

Dr. Samir Kumar Biswas   Dr. Kamal P. Singh   Dr. Ananth Venkatesan
(Supervisor)

Dated: June 14, 2020

Declaration

The work presented in this dissertation has been carried out by me under the guidance of Dr. Ananth Venkatesan at the Indian Institute of Science Education and Research Mohali.

This work has not been submitted in part or in full for a degree, a diploma, or a fellowship to any other university or institute. Whenever contributions of others are involved, every effort is made to indicate this clearly, with due acknowledgement of collaborative research and discussions. This thesis is a bonafide record of original work done by me and all sources listed within have been detailed in the bibliography.

<div align="right">

Anubhav Jindal

(Candidate)

Dated: June 14, 2020

</div>

In my capacity as the supervisor of the candidates project work, I certify that the above statements by the candidate are true to the best of my knowledge.

<div align="right">

Dr. Ananth Venkatesan

(Supervisor)

</div>

Acknowledgment

The journey of writing my MS-Thesis has been exciting and challenging. It had both ups and downs. Furthermore, through this journey, I got opportunities to interact with genuine and like-minded people who made my journey filled with enriching experiences and moments to remember. It was my first time working in a laboratory, and this gave me an opportunity to learn various experimental techniques and build up a point of view of an experimentalist.

For helping through my journey, I would like to especially thank my lab mates Mr.Shelender Kumar, Dr. Radhikesh Raveendran Angathil, Mr. Pankaj Sahu, and Mr. Shyam Sundar Yadav. They helped me to learn various experimental techniques and were always ready to help me whenever I faced an obstacle despite having a tight schedule themselves. Without their diligent help, this work could not have become more relaxed.

My sincere thanks to Dr. Ananth Venkatesan, who trusted me and gave me space in their laboratory and took me under his supervision. Whenever I had any discussion with him, I always learned something new about my work and also about being an experimentalist. I also want to thank Dr.Sanjay Mandal and his lab members for helping me out with XRD.

I would also like to thank my friends at the institute: Apoorv, Debanjan, Nikhil, Amit, Shridhar, Gaurav, Debjit, Nilangshu, Tinku, Ishan, Kabeer, Yash, Vivek, Adarsh, Swastik, Vishwas, Satyam, Himanshu with whom my time at the institute passed very quickly.

And my most sincere thanks to my parents who were always behind me, providing me a solid support during my whole life.

List of Figures

i

Abstract

Thin-film bulk acoustic wave resonators serve as an alternative to current dilelectric acoustic wave resonators for use in telecommunications [LAGG⁺11]. Because it has high resonance frequency, the current research focuses on using FBAR for sensing purposes[ZC12]. It has many advantages such as small size, IC compatibility, which makes it possible to integrate on a chip.

The FBAR has two modes for resonating: thickness extensional(TE) and thickness shear(TS). Studying these two modes is the main theme of this thesis. This thesis at first introduces the basic theory of the piezoelectric resonators and then discusses a handy equivalent circuit of the resonator called Butterworth van dyke Model.

It then dives into Finite Element Analysis of a simple geometry of both Thickness Extensional and Thickness Shear Modes of an FBAR and discusses the results that come out of it. Under the section of experimental results various recipes for depositing Aluminum Nitride are discussed and what results come out from the characterization measurements of the deposited films are discussed.

Contents

Chapter 1

Introductory Theory

1.1 Resonator Theory

The following section discusses the introductory part of the theory behind the piezoelectric resonators. It delves into the topic by discussing the propagation of waves in the non-piezoelectric slab and then modifies that solution by introducing the effects of piezoelectricity to the slab. After a certain discussion on the topic, further results are directly cited from the references mentioned. Both the thickness excitation and lateral field excitation are discussed in the following sections. This discussion is based on [Che17],[Ros88],[RD99] and [Tir10].

1.1.1 One-dimensional Equation of Motion

When an external force is applied to a deformable object, the internal structure experiences many stresses, leading to deformations called strains. Due to these internal forces, particles undergo displacement, and this leads to the definition of strain.

$$S = \frac{\partial u}{\partial z} \tag{1.1}$$

where u is particle displacement. Also the Hooke's Law gives us a relation between the stress and strain:

$$T = cS \tag{1.2}$$

where c is **Stiffness Constant**. Consider a small volume dv, the relation between the applied force and the stress is given by:

$$dF = \frac{\partial T}{\partial z} dz dA$$

Force acting on this small volume can be written as:

$$dF = dm \frac{\partial^2 u}{\partial t^2} \implies dF = \rho dz dA \frac{\partial^2 u}{\partial t^2}$$

1

where ρ is density of the solid. By equating these both equations:

$$\frac{\partial T}{\partial z} = \rho \frac{\partial^2 u}{\partial t^2} \tag{1.3}$$

By using equations 1.1,1.2,1.3 and doing some rearrangements, we get the wave equation in terms of the mechanical displacement u:

$$\frac{\partial^2 u}{\partial z^2} = \frac{\rho}{c} \frac{\partial^2 u}{\partial t^2} \tag{1.4}$$

where $v_a = \sqrt{\frac{c}{\rho}}$ is the phase velocity of the mechanical wave.

1.1.2 Solution of One Dimensional Wave Equation in Non-Piezoelectric Slab

Consider the wave equation applied to a non-piezoelectric slab which has infinite lateral dimensions(Fig:1.1a) and of lossless, isotropic and free-charge medium. Two mechanical waves propagate through the medium, the incident and reflected(Fig:1.1b). The solution of

(a) Slab with infinite lateral dimesnions   (b) Incident and reflected waves
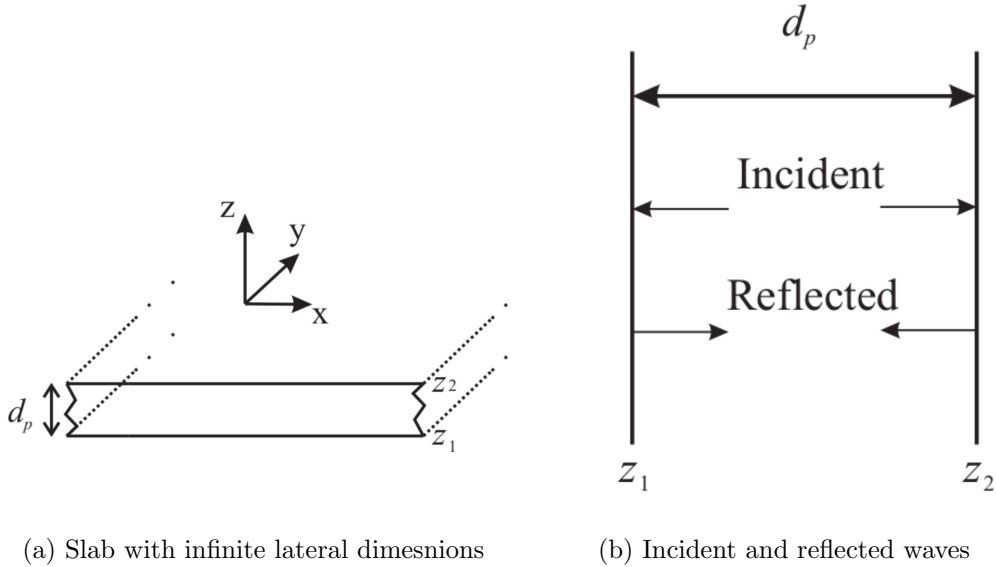
Figure 1.1: Propagation of waves in one-dimension

the mechanical wave can be written as(in phasor notation):

$$u(z) = A^+ e^{-jkz} + A^- e^{+jkz} \tag{1.5}$$

where A^+ is the amplitude of the progressive wave and A^- is the amplitude of the regressive wave. The term $k = \omega/v_a$ is the wave number, where ω is the angular frequency. At the

2

slab limits, z_1 and z_2, the particle velocity can be written as:

$$
\begin{aligned}
v_1 &= j\omega \left(A^+ e^{-jkz_1} + A^- e^{+jkz_1} \right) \\
v_2 &= j\omega \left(A^+ e^{-jkz_2} + A^- e^{+jkz_2} \right)
\end{aligned}
\tag{1.6}
$$

After some rearrangements, the amplitudes can be written as:

$$
\begin{aligned}
j\omega A^+ &= \frac{v_1 e^{jkz_2} - v_2 e^{jkz_1}}{2j \sin{(kd_p)}} \\
j\omega A^- &= \frac{v_2 e^{-jkz_1} - v_1 e^{-jkz_2}}{2j \sin{(kd_p)}}
\end{aligned}
\tag{1.7}
$$

The acoustic impedance of mechanical wave can be defined as $Z = -T/v_p$, where v_p is the particle velocity and minus sign is because T and v_p are 180° out of phase. For a plane wave solution $Z = \rho v_a$, so:

$$
T = -Z v_p = -\rho v_a v_p = -c v_p \frac{k}{\omega}
$$

In terms of applied force, $F = -AT$,

$$
F = \frac{Ackv_p}{\omega}
\tag{1.8}
$$

Also the Hooke's Law can be rewritten as:

$$
T = c\frac{\partial u}{\partial z} \implies F = jAck \left(A^+ e^{-jkz} - A^- e^{jkz} \right)
\tag{1.9}
$$

By substituting 1.7 in 1.9, the solution of the mechanical wave in a non-piezoelectric slab as a function of applied force F, the particle velocity v_p and the acoustic impedance Z is:

$$
\begin{aligned}
F_1 &= \frac{Z}{j \sin{(kd_p)}} (v_1 - v_2) + jZ \tan\left(\frac{kd_p}{2} \right) v_1 \\
F_2 &= \frac{Z}{j \sin{(kd_p)}} (v_1 - v_2) - jZ \tan\left(\frac{kd_p}{2} \right) v_2
\end{aligned}
\tag{1.10}
$$

These set of equations give a way of giving a simple circuit representation. The applied force F can be related to the voltage V and the particle velocity v to the current intensity I. The circuit model can be found in Fig:1.2. It may be related with the classical distributed T-impedance equivalent network for transmission line.[Poz09]
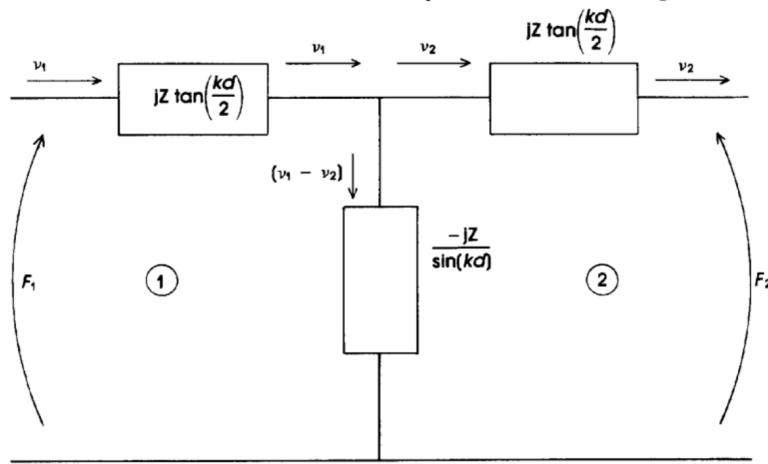
Figure 1.2: T-impedance equivalent circuit for an acoustical non-piezoelectric transmission

1.1.3 Solution of the One-Dimensional Mechanical Wave in a Piezoelectric Slab

Piezoelectricity

Piezoelectricity is the property of certain materials which deform when an electric field is applied(inverse piezoelectric effect) and alternatively, it undergoes electrical displacement when an exteral stress is applied to the material(direct piezoelectric effect).

$$D = d * T \qquad\qquad \text{(Direct)}$$
$$S = d * E \qquad\qquad \text{(Indirect)}$$

where D: Electric Displacement, T: Stress, S: Strain, E: Electric Field, d: piezoelectric constant

Since piezoelectric matrials are anisotropic, their physical constant sucha as elasticity, permittivity are tensor quantities, so we define a reference system of coordinates.(See Fig:1.3)
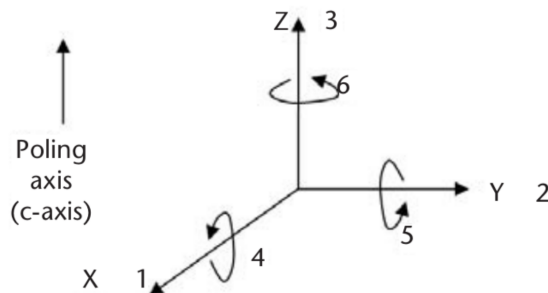

Figure 1.3: Axes Convention and directions of deformation

4

Cartesian coordinates are referred as: X-1, Y-2, Z-3, and deformation about the axis are referred as 4,5,6 respectively. The constants are generally described by two subscripts. The first subscript refers to the axis of excitation and the second one to that of actuation.

Another thing to note is that, because the velocity of electro-magnetic waves are five orders of magnitude greater than that of acoustic waves, the quasi-electrostatic approximation is valid to describe the waves travelling in piezoelectric materials. The two matrix equations that couples both elastic and electric variables of the material are given then as(involving piezoelectirc constants):

$$T_{6\times1} = c_{6\times6}^E \cdot S_{6\times1} - e_{6\times3} \cdot E_{3\times1} \tag{1.11a}$$

$$D_{3\times1} = e_{3\times6} \cdot S_{6\times1} - \varepsilon_{3\times3}^S \cdot E_{3\times1} \tag{1.11b}$$

This is known as the stress-charge form of the piezoelectric equations, where T is the stress matrix, S is the strain matrix describing the deformation of the crystal, c is the stiffness matrix, e is the piezoelectric constant matrix, E is the electric field applied to the resonator, D is the electric density displacement matrix, and ε is the permittivity matrix of the piezoelectric material. The super-script indicates that they are evaluated at constant electric field and constant strain respectively. There is an alternative strain-charge from of the above equation.

$$S_{6\times1} = s_{6\times6}^E \cdot T_{6\times1} + d_{6\times3} \cdot E_{3\times1} \tag{1.12a}$$

$$D_{3\times1} = d_{3\times6} \cdot T_{6\times1} + \varepsilon_{3\times3}^T \cdot E_{3\times1} \tag{1.12b}$$

where s is the compliance matrix and d is piezoelectric constant.

A more in depth anaysis of piezzoelectric crystals suggest due to the mechanical perturbations, the electromagnetic wave equations are modified and this analysis can be summarized as a correction to the stiffness constant, specifically c_{33}, stiffness in the thickness direction. It is:

$$c'_{33} = c_{33} + \frac{e_{33}^2}{\varepsilon_{r33}} \tag{1.13}$$

And this modiefies the phase velocity as:

$$v'_a = \sqrt{\frac{c_{33}^{'E}}{\rho}} = \sqrt{\frac{c_{33}^E + \frac{e_{33}^2}{\varepsilon_{r33}}}{\rho}} \tag{1.14}$$

Propagation of the acoustic wave through piezoelectric slab

In the piezoelectric slab, the correction terms must be applied to the mechanical parameters, so the Hooke's Law is rewritten as:

$$T = c^E \frac{\partial u}{\partial z} - eE \tag{1.15}$$

To analyze the piezoelectric slab, see Fig:1.4. The slab is excited by an electric field. For thickness excitation due to absence of any free charge, the electric displacement $\vec{D}$ remains constant, so we have:

$$\nabla \cdot \vec{D} = \rho_e = 0 \tag{1.16}$$

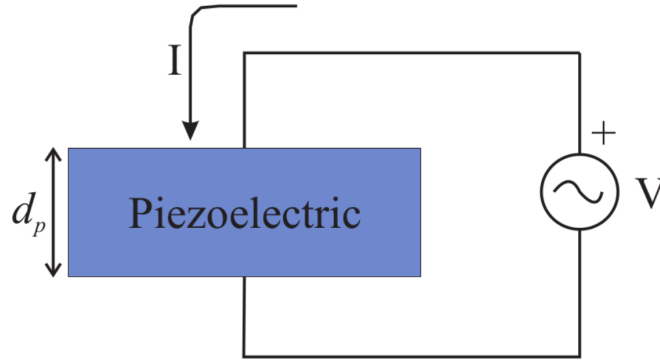For this slab, the displacement current density is,J_D is:

Figure 1.4: Thickness excitation of piezoelectric slab

$$J_D = \frac{\partial D}{\partial t} = j\omega D \Rightarrow I = j\omega DA \tag{1.17}$$

In order to obtain voltage, electric field is required and then integrated. For one-dimesional case, from 1.1 and 1.11

$$E = \frac{D}{\varepsilon^S} - \frac{e}{\varepsilon^S} \frac{\partial u}{\partial z} \tag{1.18}$$

Here first term is due to external electric field and second term is the electric field generated due to mechanical disturbances. To get voltage V, the electric field is integrated across the thickness:

$$V = \int_{z_1}^{z_2} E dz = \frac{Dd_p}{\varepsilon^S} - \frac{e}{\varepsilon^S} (u(z_1) - u(z_2)) \tag{1.19}$$

Using 1.6 in 1.19

$$V = \frac{d_p}{\varepsilon^S} \frac{I}{j\omega A} - \frac{h}{j\omega} (v_1 - v_2), \quad h = \frac{e}{\varepsilon^S} \tag{1.20}$$

By rearranging,

$$I = j\omega C_0 V + hC_0 (v_1 - v_2), \quad C_0 = \frac{\varepsilon^S A}{d_p} \tag{1.21}$$

where C_0 is the static capacitance given by the electrodes of the piezoelectric slab. There are two terms for the current in the setup, one due to the displacement field and another due to conversion of mechanical energy to electrical energy i.e piezoelectric effect. Also at the left boundary, due to piezoelectric effect, external force can be modfied as:

$$F_1 = TA = c^D SA - \frac{eD}{\varepsilon^S} A \tag{1.22}$$

Substituting 1.17 here and also applying the same modification at the other boundary, equations 1.10 can be rewritten as:

$$
\begin{aligned}
F_1 &= \frac{Z}{j\sin{(kd_p)}} (v_1 - v_2) + jZ\tan\left(\frac{kd_p}{2}\right) v_1 + \frac{h}{j\omega} I \\
F_2 &= \frac{Z}{j\sin{(kd_p)}} (v_1 - v_2) - jZ\tan\left(\frac{kd_p}{2}\right) v_2 + \frac{h}{j\omega} I
\end{aligned}
\tag{1.23}
$$

Fig 1.5shows the equivalent Mason model, an equivalent electrical circuit.(Note that there is
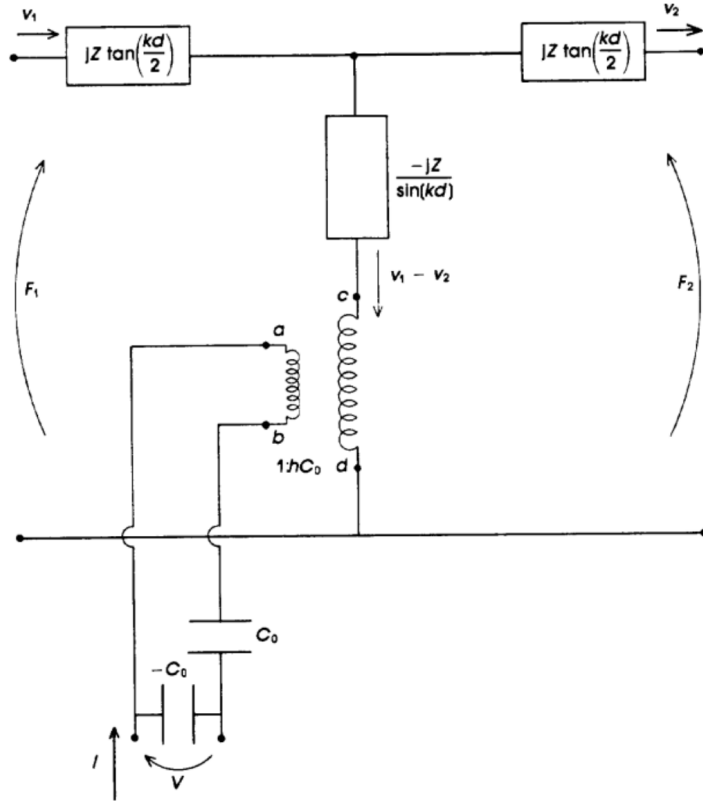

Figure 1.5: Equivalent Mason Model of Thickness Excitation in Piezoelectric Slab

a nonphysical element of negative capacitor.) The transformer is modelling the conversion of mechanical energy to electrical energy and vice-versa. As discussed in Chapter 5 and Chapter 10 [Ros88] from further analysis it can be found:

$$Z_{in} = \frac{1}{j\omega C_0} \left(1 - k_t^2 \frac{\tan(kd_p/2)}{kd_p/2}\right) \tag{1.24}$$

where,

$$C_0 = \frac{\varepsilon^S A}{d} \quad k_t^2 = \frac{e^2}{\varepsilon^S c^D} \tag{1.25}$$

Note that this is under the assumption that the metal electrodes are infintesimally small and there is no medium around the piezoelectric slab. Here Z_{in} is the input electrical impedance, k_t^2 is the electromechanical coupling coefficient and d_p is the thickness of the slab. Here two different resonances can be identified, resonance frequency that occur when $Z_{in} = 0$ and antiresonance when Z_{in} is infinite.

For antiresonance frequency,

$$Z_{in} \to \infty \Rightarrow \tan(kd_p/2) = \infty \quad \Rightarrow \quad \frac{kd_p}{2} = \frac{N\pi}{2} \quad \Rightarrow \quad \omega_a = \frac{v_p N\pi}{2d_p} \quad N = 1, 3, 5.... \tag{1.26}$$

And at resonance frequency,

$$Z_{in} \to 0 \Rightarrow k_t^2 \frac{\tan(kd_p/2)}{kd_p/2} = 1$$

As shown in Chapter 10 of [Ros88], at N^{th} pole, tangent function can be approximated as:

$$\tan\left(\frac{\theta}{2}\right) \approx \frac{4\theta}{(N\pi)^2 - \theta^2}$$

By rearrangement, the condition for resonance turns out to be:

$$\omega_r = \frac{v_a}{d_p} \left((N\pi)^2 - 8k_t^2\right)^{1/2} \tag{1.27}$$

Rearranging expressions for ω_a and ω_r, the electromechanical coupling coefficient turns out to be:

$$k_t^2 \approx \frac{\pi^2}{4} \left(\frac{\omega_a - \omega_r}{\omega_a}\right) \tag{1.28}$$

Lateral Field Excitation

For lateral field excitation, the equations are modified from the fact that electrical field $\vec{E}$ and displacement current $\vec{D}$ is the independent variable. So the mechanical equation is:

$$F = cAS - \frac{eVA}{t} \tag{1.29}$$

After analysis as shown in Chapter 10 of [Ros88], the input admittance is:

$$Y_{\text{in}} = j\omega C_0 \left(1 + K^2 \frac{\tan(kd/2)}{kd/2} \right) \tag{1.30}$$

where

$$C_0 = \frac{Wd\varepsilon^s}{t'} \quad \text{(See Fig:1.6)} \quad K^2 = \frac{e^2}{\varepsilon^S c^E} \tag{1.31}$$

At resonance frequency,

$$Y_{in} \to \infty \Rightarrow \tan(kd/2) = \infty \quad \Rightarrow \quad \frac{kd}{2} = \frac{N\pi}{2} \quad \Rightarrow \quad \omega_a = \frac{N\pi v_p}{2d} \tag{1.32}$$
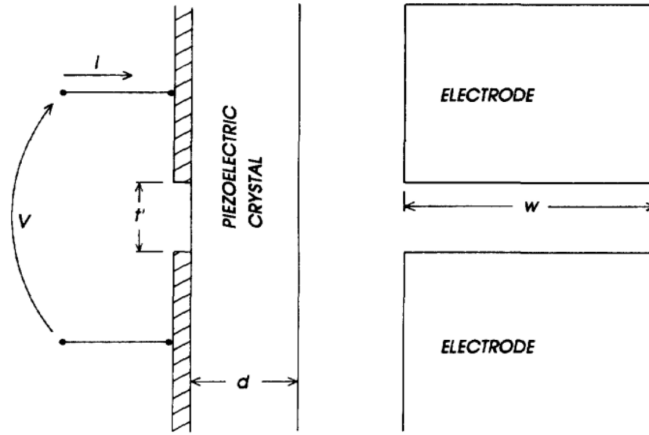

Figure 1.6: Schematic for lateral field excitation

And by similar analysis in thickness excitation section, at antiresonance frequency,

$$Y_{in} \to 0 \Rightarrow K^2 \frac{\tan(kd/2)}{kd/2} = 1 \quad \Rightarrow \quad \omega_a = \frac{v_a}{d} \left((N\pi)^2 - 8K^2 \right)^{1/2} \tag{1.33}$$

By approximating by Taylor expansion,1.33, becomes

$$K^2 \approx \frac{\pi^2}{4} \left(\frac{\omega_a - \omega_r}{\omega_a} \right) \tag{1.34}$$

Also the force equation in this can be written as, where V is the independent variable.

$$F_1 = \frac{Z}{j\sin(kd)} (v_1 - v_2) + jZ \tan\left(\frac{kd}{2}\right) v_1 + \frac{Ae}{d} V \tag{1.35}$$

So the equivalent circuit for this acoustoelectrical equation is(See Fig:1.7
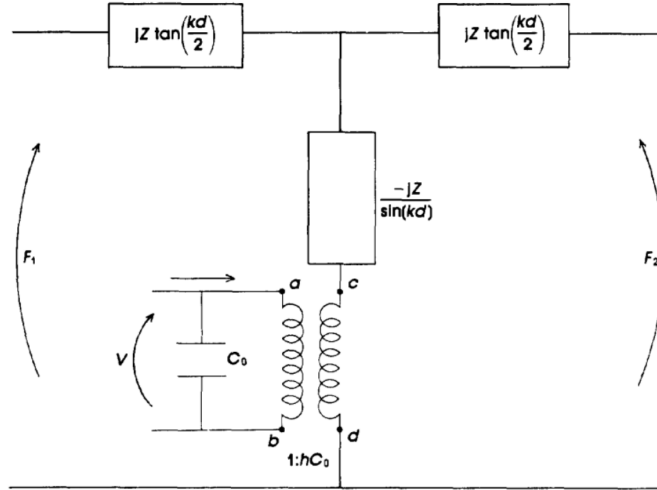
Figure 1.7: Equivalent Mason Model of LFE in piezoelectric slab

Quality Factor

The piezoelectric resonators are characterized by two factors, the electromechanical coupling coefficient and the Quality factor. It is defined as the ratio of energy stored to the energy dissipated per wave cycle. It is the function of angular frequency(ω).

$$Q = (\omega) \frac{\text{Energy stored}}{\text{Energy dissipated per wave cycle}} \tag{1.36}$$

It is the measure of the relative loss of energy in the resonator such as electrical, mechanical or acoustic. In ideal resonators since there is no energy loss, so Q is infinite but in real resonators Q is finite. Usually the quality factor is extracted from the impedance(or impedance) phase curve $\phi = \tan^{-1}\left(\frac{\text{Im}(Z)}{\text{Re}(Z)}\right)$.[LKM93]

$$Q_r = \frac{f_r}{2}\left|\frac{d\phi}{df}\right|_{f_r} \tag{1.37}$$

Chapter 2

Butterworth Van-Dyke Model

2.1   Introduction

Since the resonators are used in circuits, so it becomes beneficial to have an equivalent circuit model for the Bulk Acoustic Wave(BAW) resonator. One of the most simple ones is Butterworth Van Dyke(BVD) model. This model is lumped-element electrical equivalent circuit model that consists of an inductance(L_1), capacitance(C_1), and resistance(R_1), corresponding respectively to inertia, compliance, and damping of the mechanical system; connected in series with a parallel capacitance(C_0), which is due to the dielectric properties of the piezoelectric crystal capacitively coupled between the electrodes(See Fig:2.1).
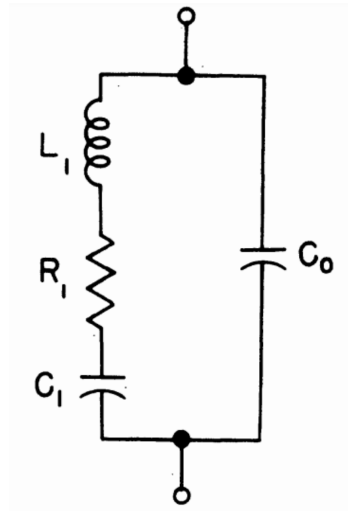

Figure 2.1: Butterworth Van Dyke Model

The representation is only useful only when the four parameters are constant and independent of frequency and amplitude[MTW+88]. The parameters are independent of frequency if the vibrator has no other mode near its resonance. The parameters vary widely between vibrators of various types and can only be determined by the experiment.

Due to the elements L_1 and C_1, there is a series resonance frequency ω_s and there is a parallel resonance frequency ω_p, set by C_0 in parallel with L_1 and C_1. All of these parameters are determined through the experiments. The electrical losses due to the electrodes can be modeled by an additional resistor of R_S included at the input.(See Fig:2.2)

However, when the BVD model is analyzed for Thin Film Bulk Acoustic Resonator(FBAR), there is a need to add an additional resistance(R_0) in series with capacitance C_0 to account for dielectric loss tangent of piezo film and models most of the losses associated with the parasitic lateral modes in FBAR[LBWR00](See Fig:2.2).
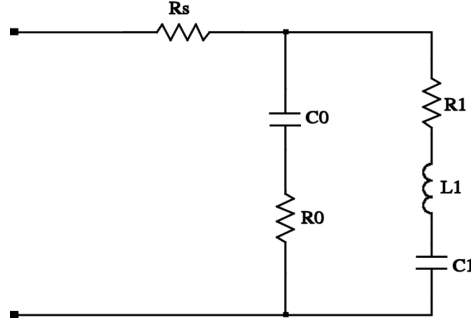

Figure 2.2: Modified Butterworth Van Dyke Model

2.2 Extraction of Parameters

For a resonator, following properties can be determined experimentally: Resonance frequency(ω_s), Anti-resonance frequency(ω_p) and their respective Quality Factors(Q_s and Q_p) by the resonators impedance analysis.From [UGY14] and [UTNG17], impedance for an FBAR can be written as:

$$Z(s) = R_s + \frac{(1 + s\tau_p)(s^2 + s\frac{\omega_s}{Q_s} + \omega_s^2)}{sC_0(s^2 + s\frac{\omega_p}{Q_p} + \omega_p^2)} \tag{2.1}$$

where $s = i\omega$ and

$$\tau_p = \frac{1}{\omega_p^2 - \omega_s^2}\left(\frac{\omega_p}{Q_p} - \frac{\omega_s}{Q_s}\right)$$

For the circuit in Fig:2.2, its impedance can be written as:

$$Z(s) = R_s + \frac{\left(sL_m + \frac{1}{sC_m} + R_m\right)\left(\frac{1}{sC_0} + R_0\right)}{\left(sL_m + R_m + R_0 + \frac{1}{sC_m} + \frac{1}{sC_0}\right)} \tag{2.2}$$

12

By rearranging (2.2) and comparing it to (2.1), we get:

$$\omega_s = \frac{1}{\sqrt{L_m C_m}} \quad Q_s = \frac{L_m \omega_s}{R_m}$$

$$\omega_p = \omega_s \left(\sqrt{1 + \frac{C_m}{C_0}} \right) \quad Q_p = Q_s \frac{\frac{\omega_p}{\omega_s}}{\left(1 + \frac{R_0}{R_m}\right)}$$

$$\tau_p = R_0 C_0$$

Since C_0 is the capacitance of the resonator, it can be directly determined experimentally, and in terms of characteristics of the resonator, the parameters of MBVD model can be written as:

$$C_m = C_0 \left[\left(\frac{\omega_p}{\omega_s}\right)^2 - 1 \right] \quad L_m = \frac{1}{\omega_s^2 C_m}$$

$$R_m = \frac{\omega_s L_m}{Q_s} \quad R_0 = R_m \left(\frac{\omega_s}{\omega_p} \frac{Q_s}{Q_p} - 1 \right)$$

Chapter 3

Simulations and Discussions

Film Bulk Acoustic Resonators(FBARs) in both its Thickness Extensional(TE) and Thickness Shear(TS) modes depend upon several parameters such as the thickness of the piezoelectric film, the material, and thickness of electrodes and so on. And Finite Element Analysis serves a very convenient method to analyze such dependencies. To analyze such dependencies, COMSOL Multiphysics®[COM] is used to simulate the FBARs. COMSOL Multiphysics provides a module on MEMS[MEM] which provides studies on Piezoelectricity. The following simulations are inspired from [Mul] and [MHES01],

Strategy for 2-D Simulation

This section outlines the general strategy to simulate a 2D FBAR via Finite Element Analysis in a software such as COMSOL Multiphysics® (See Fig:3.1):

1. **Structure of the geometry**: Define the structure of the geometry and declare variables such as piezoelectric film thickness that are being parameterized.

2. **Assigning materials to geometry**:Once the geometry is defined, the appropriate materials are assigned to different parts of the geometry. Values of intrinsic properties such as elastic modulus, dielectric constant etc. are already stored in the materials.

3. **Setting boundary conditions for both Electrostatics and Solid Mechanics**: Fixed constraint is applied to the appropriate edges of the geometry. The electrodes are kept at Ground and Voltage Terminal respectively.

4. **Applying Losses to the materials**: Losses such as Mechanical Damping and dielectric losses are defined for the appropriate material.

5. **Meshing the geometry**: Geometry of FBAR is meshed in such as way that the area around piezoelectric film and electrodes is finely meshed and area around Silicon and Silicon Nitride is coarsely meshed in comparison.

6. **Choosing the Study**: The analysis is done by choosing the Frequency Domain Study from the repository. Impedance curves are plotted and are then further analyzed.

3.1 Thickness Excitational Mode

In thickness excitational mode the major factors that effect the resonance frequencies and their quality factors are thickness of the piezoelectric film, material of the electrodes and the thickness of the electrodes. Each of these factors is simulated and the results discussed. The general geometry employed in these simulations is shown in Fig:3.1
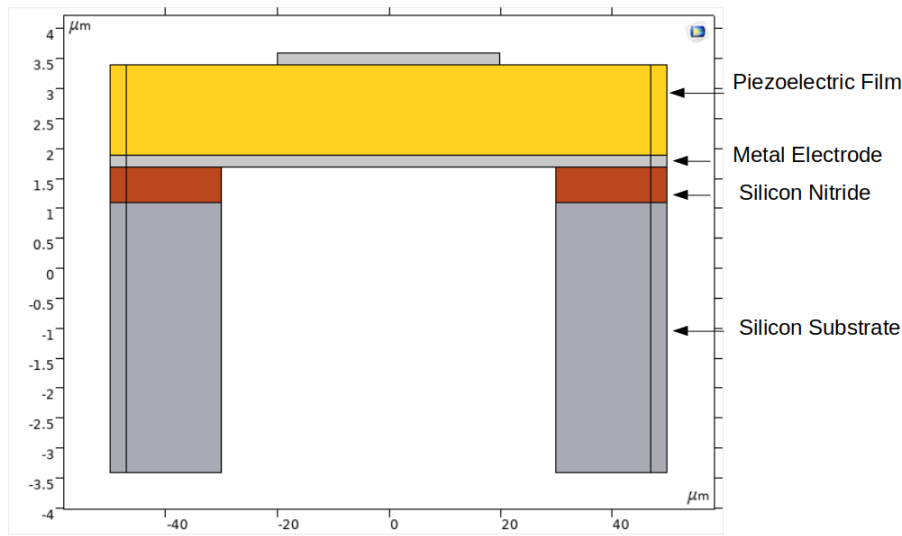

Figure 3.1: Schematic of TE FBAR

3.1.1 Dependence on Thickness of Piezoelectric Film

To measure the dependence of film thickness on resonance and anti-resonance frequencies, frequency analysis is run for thickness ranging from $1\mu m$ to $3\mu m$ and the peaks are identified for the first harmonics in both resonance and anti-resonance. From Fig3.2a it can been seen that these frequencies are inversely proportional to the thickness of the film as the theory predicts. As for the dependence of the parameters such as Quality factor(Fig:3.2b) and Effective Electromechanical Coupling(Fig:3.2c) there is no visible dependence just on the thickness of the piezoelectric film.

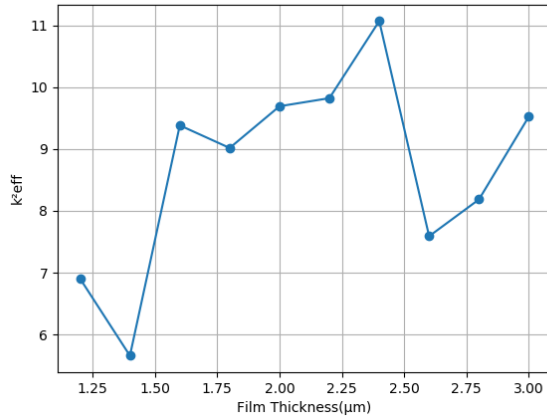### 3.1.2 Dependence on Electrode Thickness

By keeping the thickness of the piezoelectric film to be around $1\mu m$ and the electrode material to be Aluminum, frequency analysis is conducted for electrode thickness to be ranging
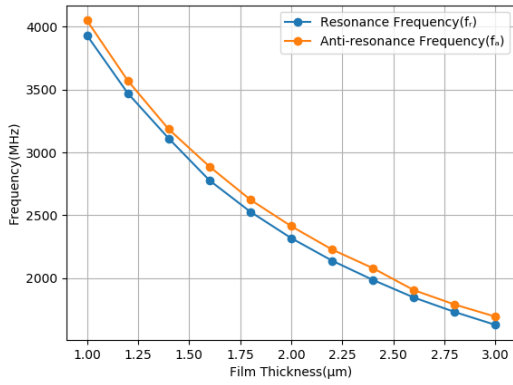
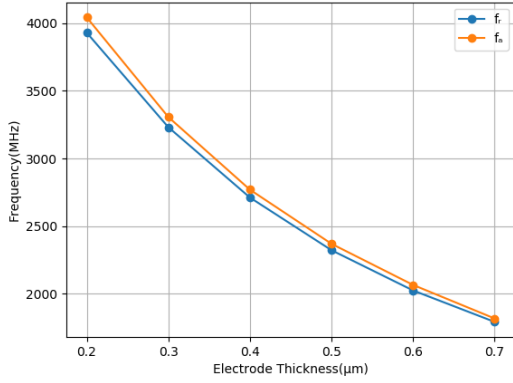(a) Dependence of Frequencies on Film Thickness
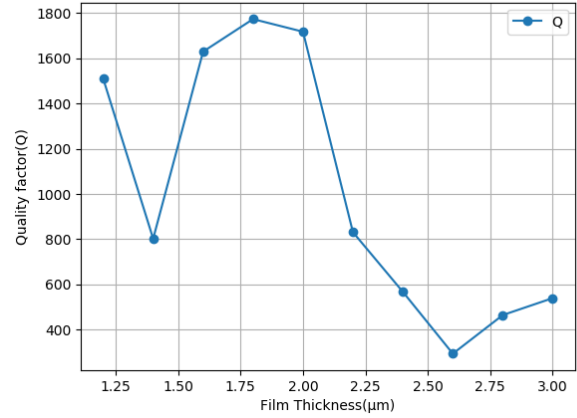
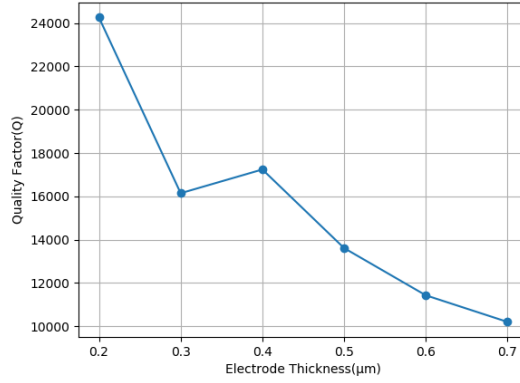(b) Quality Factor vs Film Thickness

(c) Effective Electromechanical Coupling vs Film
Thickness

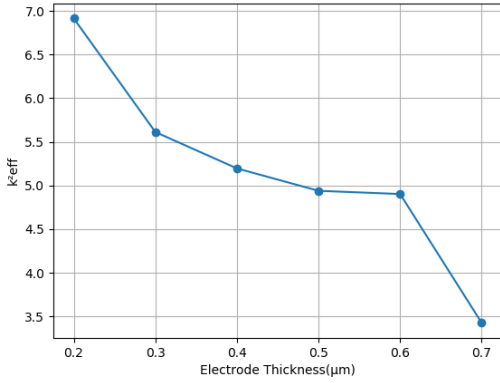Figure 3.2: Parameters dependence on Film Thickness

from $0.2\mu m$ to $0.7\mu m$. Resonance and anti-resonance frequencies are identified and then the quality factor and effective electromechanical coefficient is calculated.

From Fig:3.3a it can seen that as the electrode thickness is increased, the resonance and anti-resonance frequencies decrease[ICO$^+$08]. But also in terms of quality factor and effective electromechanical coefficient there the trend also seems to be inversely proportional to the electrode thickness(See Fig:3.3b, Fig:3.3c). This is experimentally verified in [LBMM01] which suggested a technique in which they keep etching the electrode layer and kept making the measurements.

(a) Dependence of Resonance and Anti-resonance Frequencies on Electrode Thickness

(b) Quality Factor vs Electrode Thickness

(c) Effective Electromechanical Coupling vs Electrode Thickness

Figure 3.3: Parameters dependence on Electrode Thickness

3.2   Lateral Field Excitation

Lateral field excitation is one of the ways of producing thickness shear mode in the piezoelectric film. The major factors that effect the resonance frequencies and their quality factors are thickness of the piezoelectric film, seperation between the electrodes, and thickness of the metal electrodes. Each of these factors is simulated and the results discussed. The schematic of the geometry is shown in Fig:3.4.

3.2.1   Dependence on Electrode Seperation

Seperation between electrodes play a major role in effecting the quality of the peaks of the resonance frequencies. From Fig:3.5 it can be seen that as the seperation between the electrodes increases the peaks at resonance and antiresonance becomes more prominent. This arises due the fact that, when the seperation between the electrodes is small, more part
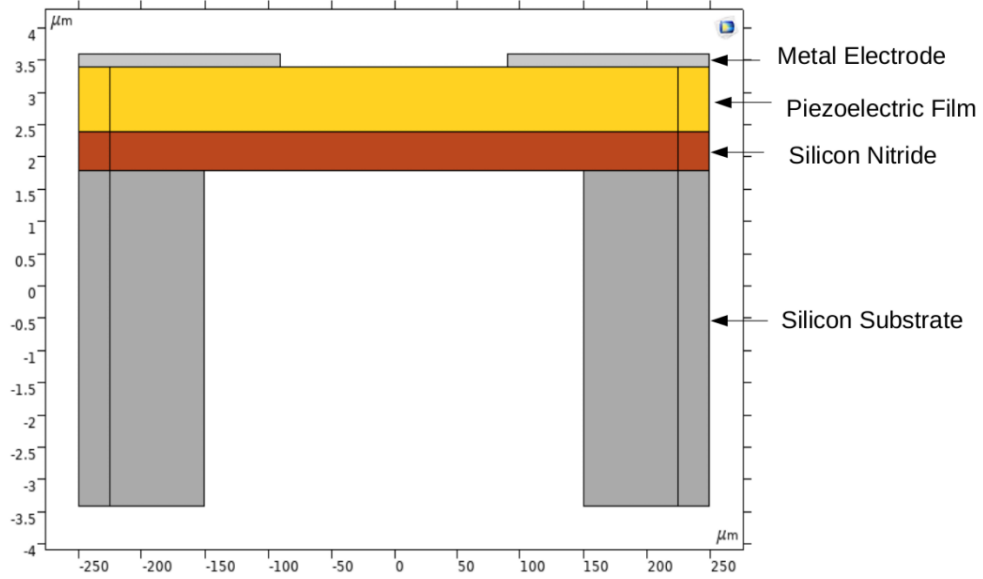
18

Figure 3.4: Schematic of LFE FBAR

of the electric field in the piezoelectric material is not parallel to the the lateral dimension of the film whereas when the seperation is large enough major part of the electric field is in lateral dimension of the piezoelectric film[CWL+10].(See Fig:3.6a and 3.6b). The experimental verifications and further discussions can be found in [CIO+12],[GRB+11]

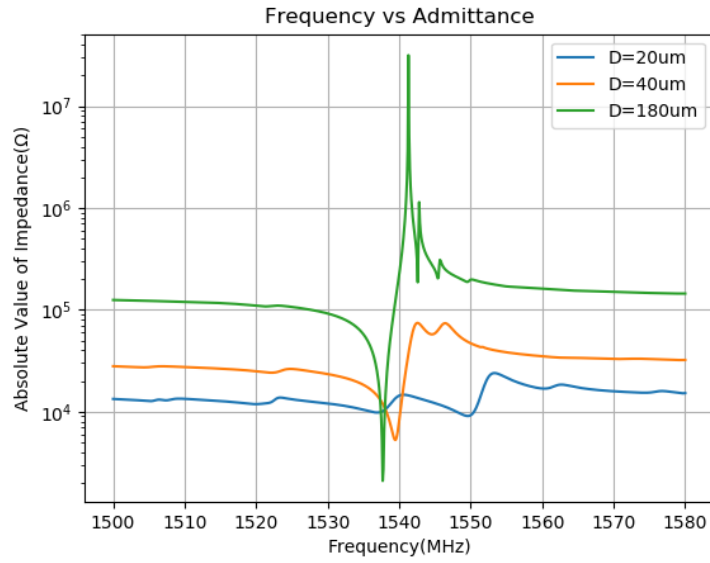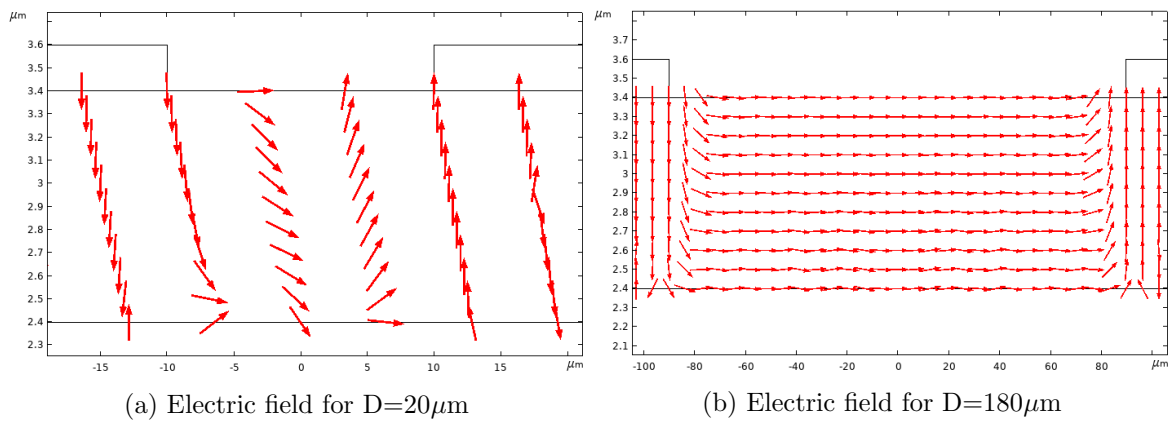19

Figure 3.5: Frequency vs Admittance for different electrode seperation

(a) Electric field for D=20μm


(b) Electric field for D=180μm

Figure 3.6: Electric field pattern for different electride seperation

20

3.2.2 Dependence on Thickness of the Film

Film thickness has the same effect as seen in the case for thickness extensional mode. The thickness of the film is varied from $1\mu m$ to $3\mu m$ and the trends in resonance and antiresonance frequencies are noticed.
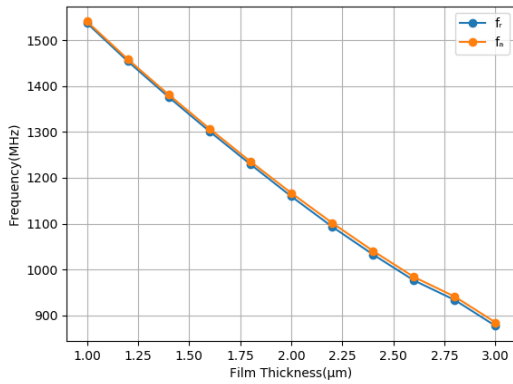
(a) Thickness dependence of Charcteristic Frequencies
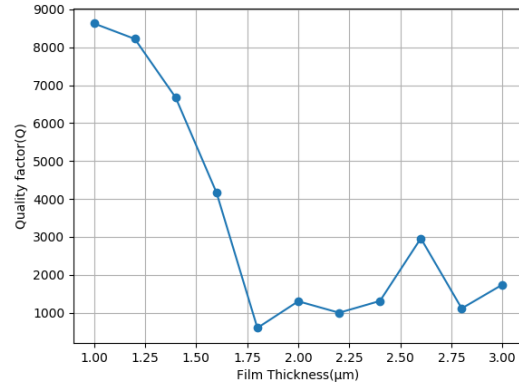
(b) Thickness dependence of Quality factor
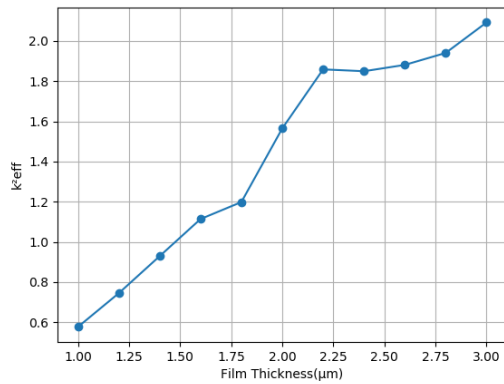
(c) Thickness dependence of Effective Electromechanical Coefficient

Figure 3.7: Dependence of Parameters on Thickness

The resonance and antiresonance frequencies vary inversely to the thickness of the film, whereas quality factor varies independently to the thickness of the film. Here effective electromechanical coefficient varies directly proportional to the thickness of the film.

Chapter 4

Experimental Results and Discussions

Zinc Oxide and Aluminum Nitride are two very promising candidates for the piezoelectric material used in FBAR. However, Aluminum Nitride is a better material due to its various advantages such as high bulk acoustic wave velocity, moderate electromechanical coupling, high electric resistivity, low dielectric loss, good chemical, and thermal stability and wide band gap[CCCH07]. All these properties arise due to its structure.(See Fig:4.1)

(a) Hexagonal Structure of Aluminum Nitride

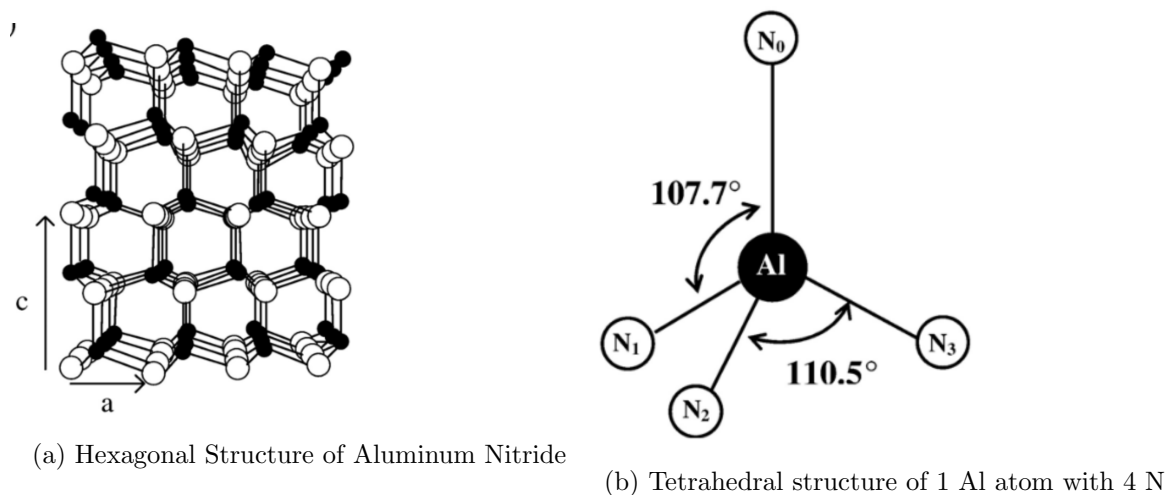(b) Tetrahedral structure of 1 Al atom with 4 N

Figure 4.1: Structure of Aluminum Nitride

There are numerous methods for depositing Aluminum Nitride, but the most proficient technique is RF Magnetron Sputtering. Several recipes are discussed in [IMY18], but due to constraints, the recipes that were employed had room temperature as substrate temperature.

4.1 Studying the deposition of Aluminum Nitride on Silicon Substrate

The Sputtering Deposition apparatus available in the lab allows us to control the following parameters: RF and DC Power, Pressure, Flow of Air(such as N_2 and Ar). The thermostat, which controlled the temperature of the substrate, is not working. So with varying the parameters as mentioned earlier and varying the time for deposition, several samples were prepared to study the effect of these parameters on the quality of the Aluminum Nitride thin film deposited. The first set of samples were prepared with depositing Aluminum Nitride on Silicon surface. The following range of parameters was set for these samples.

RF Power(W)	Sputtering Pressure(mTorr)	N_2/Ar Ratio(%)	Time(min)
$60, 90, 120$	$4.9 - 5.9$	$40, 50, 60, 80$	$10, 20, 30, 45, 60$

Though many samples were prepared but were not analyzed with X-Ray Diffraction because of its rare availability. But with the samples analyzed following observations were made:

4.1.1 X-Ray Diffraction Observations

Around three samples were analyzed where Aluminum Nitride thin films were deposited on a Silicon substrate. Figure 4.2 demonstrates that there is no peak that corresponds to any of the peak of Aluminum Nitride. Similar features were seen in the other two samples.

Sample 1	60W,20min, 50%,5.2mTorr
Sample 2	60W,20min, 60%,5.2mTorr
Sample 3	60W,20min, 80%,5.2mTorr

4.1.2 SEM

Scanning Electron Microscope was employed to measure the thickness of the Aluminum Nitride thin film deposited on the substrate and also look at the grain structure of AlN crystals. The samples were inserted in such a way that the cross-section of the thin film can be looked. Before inserting the sample, the Silicon chip was cut, so a fine view of the crystals was available. Figure4.3 shows that the Aluminum Nitride film has a columnar structure. Moreover, from most of the samples, it was found that the thin film thickness deposited on Silicon did not exceed 400nm.
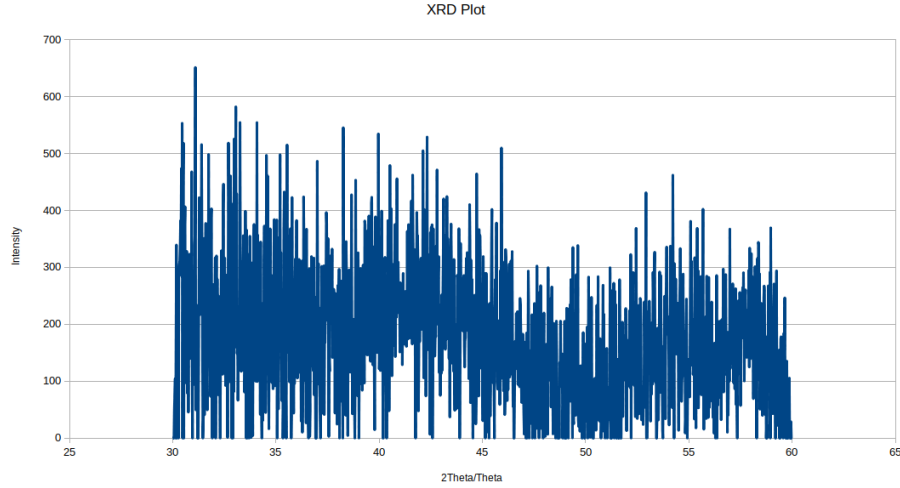
Figure 4.2: XRD Plot of Sample 1

4.2 Studying the deposition of Aluminum Nitride on Molybdenum layer

The layer of Molybdenum was deposited on Silicon chip of thickness 200nm via DC Sputtering. The parameters of the system were following:

DC Power(W)	Sputtering Pressure(mTorr)	Ar Flow Rate(sccm)	Time(min)
40	10	20	20

A batch of such chips were prepared and Aluminum Nitride was deposited on these chips by varying the the parameters.

RF Power(W)	Sputtering Pressure(mTorr)	N_2/Ar Ratio(%)	Time(min)
60	$4.9 - 5.9$	$40, 50, 60$	$10, 20, 30$

Among these samples only few of them were analyzed with XRD.

4.2.1 X-Ray Diffraction Observation

Around two samples were analyzed where Aluminum Nitride thin film was deposited on a Mo layer on the Silicon substrate. Fig:4.4 shows that XRD only identifies Molybdenum, whereas Aluminum Nitride is still missing.

Sample 1	60W,20min, 10%,5.2mTorr
Sample 2	60W,20min, 20%,5.2mTorr

Since the deposited layer of Aluminum Nitride is supposedly very thin for XRD to identify. However, since Molybdenum is a massive element, it was still identified despite its thickness to be very low. Also, Aluminum Nitride might be deposited because the Molybdenum
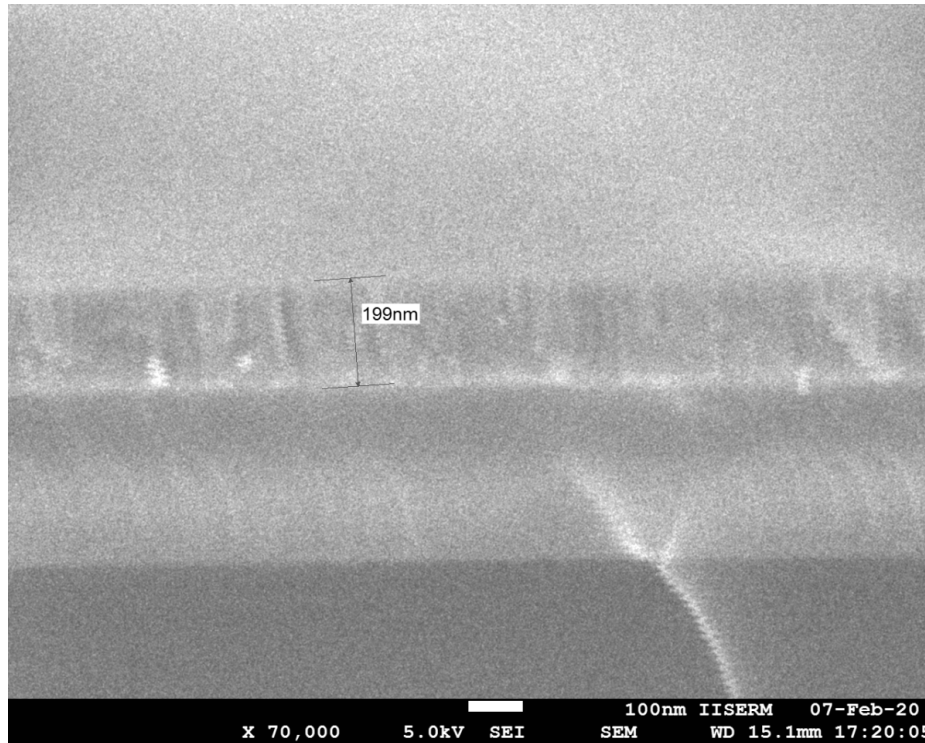
25

Figure 4.3: XRD Plot of Sample$(60W, 10min, 50\%.5.2mTorr)$

layer is conducting. In contrast, Aluminum Nitride is an insulator, and after checking the resistance, the chips were found to be an insulator.
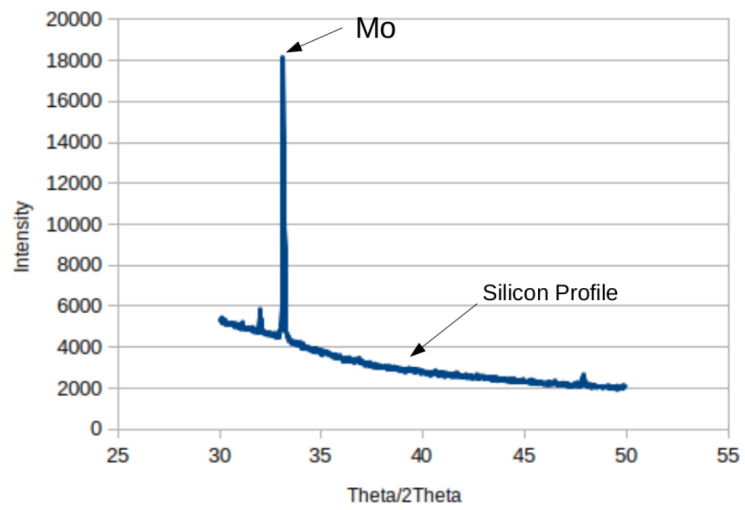
Figure 4.4: XRD of Sample 1

Appendix A

Fabrication of Sample Holder

The following work is a side project in which I had to fabricate a sample holder for the Dilution Refrigerator in Ultra-Low Temperature Physics Lab. The purpose of this sample holder is to hold a minimum of three samples during a single cooldown of the refrigerator. This holder is prepared using **Photolithography**. The design (see Fig:A.1) of the holder is made using a CAD software called **EagleCAD**. The process is described below:
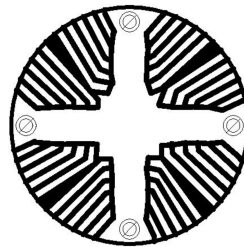
Figure A.1: Sample Holder Design

Materials required: Photoresist film, Copper Clad Board, Laminator, UV Exposure Box, Sodium Carbonate(Developer), Ferric Chloride(Copper Etchant), Sodium Hydroxide(Photoresist Remover)

Procedure

- Clean the Copper Clad Board with a scrub, so that there is a clean surface on top.(See Fig:A.2a)

- Cut a piece of the photoresist film, remove the protective layer and place the film carefully on the clad without touching the resist side of the film.(See Fig:A.2b)

- Using heat from the laminator resist is transferred on the clad.

29

- Place the OHP sheet, on which the design is printed, on the clad and place it in the UV Exposure Box for 5 minutes.

- Since the film is negative, when the resist is developed, the unexposed part will be removed while the exposed part retains on the clad.

- Developer is prepared by 5mg of Na_2CO_3 in 100ml of water. Place the clad in this developer and shake till the unexposed part is removed from the clad, leaving the copper on that part exposed for etching.(See Fig:A.2c)

- Prepare the etchant solution of 0.4mg/ml solution of $FeCl_3$ and place the clad in this solution. The etchant removes copper from the exposed part.

- Prepare the resist remover solution with 0.07mg/ml solution of NaOH and place the clad in this solution. This removes the resist from the rest of the clad. And now we have the required sample holder.(See Fig:A.2d)

(a) Copper Clad
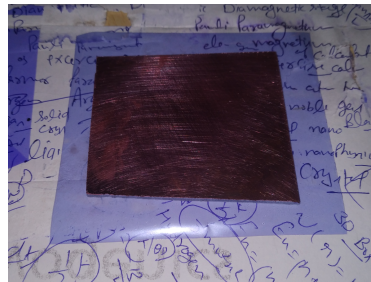
(b) Photoresist film on clad

(c) Developed pattern

(d) Sample Holder

Figure A.2: Process in Pictures

Bibliography

[CCCH07]   Kuan-Hsun Chiu, Jiann-Heng Chen, Hong-Ren Chen, and Ruey-Shing Huang, *Deposition and characterization of reactive magnetron sputtered aluminum nitride thin films for film bulk acoustic wave resonator*, Thin Solid Films **515** (2007), no. 11, 4819–4825.

[Che17]   J David N Cheeke, *Fundamentals and applications of ultrasonic waves*, CRC press, 2017.

[CIO$^+$12]   M Clement, E Iborra, J Olivares, M de Miguel-Ramos, J Capilla, and J Sangrador, *On the lateral excitation of shear modes in aln layered resonators*, 2012 IEEE International Ultrasonics Symposium, IEEE, 2012, pp. 1–4.

[COM]   *COMSOL Multiphysics Reference Manual, version 5.5, COMSOL, Inc, www.comsol.com*.

[CWL$^+$10]   Da Chen, Jingjing Wang, Dehua Li, Luyin Zhang, and Xueshui Wang, *The c-axis oriented aln solidly mounted resonator operated in thickness shear mode using lateral electric field excitation*, Applied Physics A **100** (2010), no. 1, 239–244.

[GRB$^+$11]   M Gorisse, A Reinhardt, C Billard, M Borel, E Defaÿ, T Bertaud, T Lacrevaz, and C Bermond, *Lateral field excitation of membrane-based aluminum nitride resonators*, 2011 Joint Conference of the IEEE International Frequency Control and the European Frequency and Time Forum (FCS) Proceedings, IEEE, 2011, pp. 1–5.

[ICO$^+$08]   E. Iborra, M. Clement, J. Olivares, S. Gonzalez-Castilla, J. Sangrador, N. Rimmer, A. Rastogi, B. Ivira, and A. Reinhardt, *Baw resonators based on aln with ir electrodes for digital wireless transmissions*, 2008 IEEE Ultrasonics Symposium, 2008, pp. 2189–2192.

[IMY18]   Abid Iqbal and Faisal Mohd-Yasin, *Reactive sputtering of aluminum nitride (002) thin films for piezoelectric applications: A review*, Sensors **18** (2018), no. 6, 1797.

[LAGG$^+$11]   JK Luo, GM Ashley, L Garcia-Gancedo, PB Kirby, AJ Flewitt, and WI Milne, *Film bulk acoustic resonator nanosensors for multi-task sensing*, International Journal of Nanomanufacturing **7** (2011), no. 5-6, 448–462.

[LBMM01]   K. M. Lakin, J. Belsick, J. F. McDonald, and K. T. McCarron, *Improved bulk wave resonator coupling coefficient for wide bandwidth filters*, 2001 IEEE Ultrasonics Symposium. Proceedings. An International Symposium (Cat. No.01CH37263), vol. 1, 2001, pp. 827–831 vol.1.

[LBWR00]   John D Larson, Paul D Bradley, Scott Wartenberg, and Richard C Ruby, *Modified butterworth-van dyke circuit for fbar resonators and automated measurement system*, 2000 IEEE Ultrasonics Symposium. Proceedings. An International Symposium (Cat. No. 00CH37121), vol. 1, IEEE, 2000, pp. 863–868.

[LKM93]   K. M. Lakin, G. R. Kline, and K. T. McCarron, *High-q microwave acoustic resonators and filters*, IEEE Transactions on Microwave Theory and Techniques **41** (1993), no. 12, 2139–2146.

[MEM]   *MEMS Module User's Guide,COMSOL Multiphysics$^{®}$,version 5.5,COMSOL,Inc, www.comsol.com*.

[MHES01]   T. Makkonen, A. Holappa, J. Ella, and M. M. Salomea, *Finite element simulations of thin-film composite baw resonators*, IEEE Transactions on Ultrasonics, Ferroelectrics, and Frequency Control **48** (2001), no. 5, 1241–1258.

[MTW^{+}88]   A Meitzler, H Tiersten, A Warner, D Berlincourt, G Couqin, and F Welsh III, *176-1987-ieee standard on piezoelectricity*, IEEE Ultrasonics, Ferroelectrics, and Frequency Control Society (1988).

[Mul]   COMSOL Multiphysics$^{®}$, *Thin Film BAW Composite Resonator.version 5.5,COMSOL,Inc, www.con*

[Poz09]   David M Pozar, *Microwave engineering*, John Wiley & Sons, 2009.

[RD99]   Daniel Royer and Eugene Dieulesaint, *Elastic waves in solids i: Free and guided propagation*, Springer Science & Business Media, 1999.

[Ros88]   Joel Rosenbaum, *Bulk acoustic wave theory and devices*, Artech House on Demand, 1988.

[Tir10]   Jordi Verdú Tirado, *Bulk acoustic wave resonators and their application to microwave devices*, PhD, Universitat Antonoma de Barcelona (2010).

[UGY14]   Ivan Uzunov, Dobromir Gaydazhiev, and Ventsislav Yantchev, *Lattice fbar filters: Basic properties and opportunities for improving the frequency*, Journal of Communications **2** (2014), no. 4, 103–117.

[UTNG17]   Ivan S Uzunov, Milena D Terzieva, Boyanka M Nikolova, and Dobromir G Gaydazhiev, *Extraction of modified butterworthvan dyke model of fbar based on fem analysis*, 2017 XXVI International Scientific Conference Electronics (ET), IEEE, 2017, pp. 1–4.

[ZC12]   Yafei Zhang and Da Chen, *Multilayer integrated film bulk acoustic resonators*, Springer Science & Business Media, 2012.